



ELSEVIER

Physica D 135 (2000) 63–78

PHYSICA D

www.elsevier.com/locate/physd

Detecting switch dynamics in chaotic time-waveform using a parametrized family of nonlinear predictors

Isao Tokuda^{a,*}, Ryuji Tokunaga^b, Takashi Matsumoto^c

^a Department of Computer Science and Systems Engineering, Muroran Institute of Technology, Hokkaido 050-8585, Japan

^b Institute of Information Sciences and Electronics, University of Tsukuba, Ibaraki 305-8573, Japan

^c Department of Electrical, Electronics and Computer Engineering, Waseda University, Tokyo 169-8555, Japan

Received 9 December 1998; received in revised form 10 March 1999; accepted 10 April 1999

Communicated by M. Sano

Abstract

An algorithm is presented for detecting switch dynamics in chaotic time-waveform. By the “switch dynamics,” we mean that the chaotic time-waveform is measured from a dynamical system whose bifurcation parameters are occasionally switched among a set of slightly different parameter values. First, the switched chaotic time-waveform is divided into windows of short-term time-waveforms. From the set of windowed time-waveforms, “qualitatively similar” parametrized family of nonlinear predictors is constructed. “Qualitatively similar” parametrized family means that the family of nonlinear predictors exhibits “qualitatively similar” bifurcation phenomena as the original. By characterizing the windows of short-term chaotic time-waveforms in terms of the “qualitative” parameters of nonlinear predictors, switch dynamics of their associated bifurcation parameters are detected. For the Lorenz equations, the Rössler equations, and the Mackey–Glass equations, efficiency of the algorithm is demonstrated. In the experiment, chaotic time-waveforms contaminated with observational noise is considered. ©2000 Elsevier Science B.V. All rights reserved.

PACS: 47.52.+j

Keywords: Chaos; Bifurcation; Chaotic time-waveform; Switch dynamics; Non-stationarity; Parametrized family of nonlinear predictors

1. Introduction

In the studies of chaotic time-waveform analyses [1–11], it has been supposed that the time-waveform is stationary and the bifurcation parameters of the underlying chaotic dynamical system are not changed. Such chaotic time-waveforms can be characterized by the statistical property of the underlying chaotic dynamics such as fractal dimension [2], Lyapunov exponents [3–5], Kolomogorov–Sinai entropy [6], and nonlinear predictability [7–11]. In practice, however, bifurcation parameters of the time-waveforms measured from real-world systems can be occasionally changed. For example, in the flow dynamics, the system variables are sometimes composed of the fast-dynamic

* Corresponding author. Tel.: +81-143-46-5477; fax: +81-143-46-5499
E-mail address: tokuda@muroran-it.ac.jp (I. Tokuda)

components and the slow-dynamic ones [12]. The dominant fast-dynamic patterns are occasionally changed by the slow-dynamic variables, which can be considered as the occasionally changed bifurcation parameters.

The occasional change in the bifurcation parameters can also have a functionality for transmitting binary code information. For example, human speech with binary word information is transmitted by the sequential changes in the oscillatory states of the vocal system. Another example is the chaotic secret communication systems [13–15]. This communication system is composed of transmitter subsystem and receiver subsystem. With a successive change between two bifurcation parameter values, p_+ and p_- , the transmitter subsystem exhibits switch dynamics among the two chaotic attractors associated with p_+ and p_- . By the Pecora–Carroll synchronization [16,17], the switch dynamics of the transmitter is sent to the receiver and the binary information encoded as a sequence of the switched bifurcation parameters can be decoded in the synchronized receiver subsystem.

For the analyses of chaotic time-waveforms with such switched bifurcation parameters, conventional techniques for analyzing chaotic time-waveforms cannot be directly applied. This is because the conventional techniques [1–11] mainly estimate statistical properties of the underlying chaotic dynamics from long enough time-waveform data with fixed bifurcation parameters. Towards the analyses of chaotic time-waveforms with switched bifurcation parameters, various new numerical algorithms have been recently developed [18–24]. The basic numerical procedure for analyzing switch dynamics in chaotic time-waveform is to first divide a time-waveform into windows of short-term time-waveform data. Then dynamical closeness between the windows of the data are measured by computing the difference in statistical quantity between the windowed data such as invariant measure [18,23,24], cross-correlation integral [19,22], recurrence plot [19,20], and cross prediction error [21]. Based on the statistical test which detects a significant change in the statistical quantity of the chaotic time-waveform, the stationarity of the data can be examined.

Although these algorithms have been successfully applied to various chaotic time-waveforms with switched bifurcation parameters, there might be some limitations due to the following problems:

1. If the switch interval of the bifurcation parameters is short, reliable estimation of the statistical quantities from such short-term data cannot be always expected.
2. If the switched bifurcation parameter values are closely located with others and if the time-waveform data is contaminated with observational noise, qualitative dynamics as well as the statistical properties of the associated chaotic attractors might be similar to each other and hence detection of a slight change in the statistical property of the switched chaotic time-waveforms is quite difficult.

Our approach to the problem is rather different from the techniques of [18–24]. Since the qualitative change in the chaotic time-waveform is induced by the switch in the bifurcation parameter values, it is natural and more efficient to detect the switch dynamics by estimating the underlying switched bifurcation parameters.

The problem for estimating the underlying bifurcation parameters from chaotic time-waveforms has been studied in [25,26]. Since it is supposed that there is no information about the functional form of the parameterized family of chaotic dynamics, estimation of the exact bifurcation parameter values only from time-waveforms is impossible. Instead, “qualitatively similar” bifurcation parameter values can be estimated by a simple algorithm using a parametrized family of nonlinear predictors. The “qualitatively similar” bifurcation parameters mean that the parameters give rise to a family of nonlinear predictors which exhibits qualitatively similar bifurcation phenomena as the original. The algorithm has been successfully applied to the Hénon family, the coupled logistic/delayed-logistic family, and the Rössler family [25,26].

Based on the estimation technique of the underlying bifurcation parameters, this paper presents an algorithm for detecting switch dynamics in chaotic time-waveform. Using three typical chaotic dynamical systems, the Lorenz equations, the Rössler equations, and the Mackey–Glass equations, efficiency of the algorithm is demonstrated. In the experiments, switched chaotic time-waveforms contaminated with observational noise is considered.

2. Algorithm for detecting switch dynamics in chaotic time-waveform

2.1. Problem formulation

Consider a continuous-time chaotic dynamical system

$$\frac{d\eta_t}{dt} = f(p(s(t)), \eta_t), \quad p \in R^m, \quad \eta_t \in R^D, \quad (2.1)$$

and its observation:

$$\{\xi_t = g(\eta_t) | 0 \leq t \leq C\}, \quad (2.2)$$

where the bifurcation parameter $p(s(t))$ is occasionally changed among I -different sets of parameter values $\{p(i)\}_{i=0,1,\dots,I-1}$ by the switch signal $s(t)$,

$$s(t) = \begin{cases} 0 & \text{for } t \in V_0 \ (\subset [0, C]) \\ 1 & \text{for } t \in V_1 \\ \vdots & \\ I-1 & \text{for } t \in V_{I-1} \end{cases} \quad (2.3)$$

where $\bigcup_{i=0}^{I-1} V_i = [0, C]$ and $V_i \cap V_j = \emptyset$ for $i \neq j$.

Here we assume the following:

1. The functional form of the parametrized family of vector fields $f : R^m \times R^D \rightarrow R^D$ is not known; f is assumed to be smooth.
2. The functional form of $g : R^D \rightarrow R^1$ is not known; g is assumed to be smooth.
3. $D = \dim \eta_t$ is not known.
4. $m = \dim p$ and the sets of parameter values $\{p(i)\}_{i=0,\dots,I-1}$ are not known; $\{p(i)\}_{i=0,\dots,I-1}$ are closely located with each other.

Under the conditions (1)–(4), we consider an algorithm for detecting switch dynamics of the bifurcation parameters p in the chaotic time-waveform $\{\xi_t | 0 \leq t \leq C\}$. The algorithm is composed of four steps. First, observational noise in the measured time-waveform is smoothed out by an averaging filter, and high-dimensional chaotic trajectory is reconstructed using the delay-coordinate method. Second, the chaotic trajectory is divided into windows of short-term trajectories, and nonlinear predictors which model the windowed chaotic trajectories are constructed within a same parametrized family. Third, effective bifurcation parameters are extracted from the many parameters of the nonlinear predictors by principal component analysis. Fourth, windows of shorter-term chaotic trajectories are characterized by the principal bifurcation parameters of the nonlinear predictors and the switch dynamics in the principal bifurcation parameters are detected by the Linde–Buzo–Gray (LBG) clustering algorithm.

2.2. Averaged filtering and delay-coordinate embedding

In laboratory experiments, time-waveforms are usually sampled digitally and also contaminated with observational noise. Hence, let us rewrite Eq. (2.2) by

$$\{\xi_n = g(\eta_{n\Delta t}) + v_n | n = 1, 2, \dots, N_{\text{data}}\}, \quad (2.4)$$

where Δt is the sampling rate, N_{data} is the number of data, and v_n is Gaussian noise.

In order to smooth out the observational noise, an averaging filter is applied to the time-waveform as

$$\left\{ \hat{\xi}_n = \frac{1}{W+1} \sum_{k=n}^{n+W} \xi_k \mid n = 1, 2, \dots, N_{\text{data}} - W \right\}, \quad (2.5)$$

where W is the window length of the moving average.

From the filtered time-waveform $\{\hat{\xi}_n \mid n = 1, 2, \dots, N - W\}$, a d -dimensional trajectory $\{X_n \mid n = 1 + (d - 1)\tau, \dots, N_{\text{data}} - W\}$ is reconstructed by using a delay-coordinate [27,28]:

$$X_n = {}^T ({}^1x_n, {}^2x_n, \dots, {}^dx_n) = {}^T (\hat{\xi}_n, \hat{\xi}_{n-\tau}, \dots, \hat{\xi}_{n-(d-1)\tau}), \quad (2.6)$$

where T denotes transposition and τ denotes a time lag. The filtered delay embedding prevalence theorem [28] guarantees that the reconstructed trajectory $\{X_n\}$ is qualitatively the same as the original $\{\eta_t\}$.

2.3. Nonlinear predictors

In order to detect qualitative change in the reconstructed trajectory $\{X_n\}$, we divide the trajectory $\{X_n\}$ into J -windows of short-term trajectories with T -interval:

$$\{X_n(i) = X_n \mid n = 1 + (d - 1)\tau + (i - 1)T, \dots, (d - 1)\tau + iT\}_{i=1,2,\dots,J}. \quad (2.7)$$

For each windowed trajectory, $\{X_n(i)\}_{i=1,2,\dots,J}$, we construct a nonlinear predictor $F : R^L \times R^d \rightarrow R^d$ which model the trajectory dynamics as

$$X_{n+1}(i) \approx F(\Omega(i), X_n(i)), \quad (2.8)$$

where $\Omega \in R^L$ stands for a set of parameters of nonlinear predictor $F(\cdot, \cdot)$. Among a variety of functional forms for nonlinear predictors such as polynomial functions [7], radial basis functions [10], multi-layer perceptrons (MLP) [9], MLP is chosen as a nonlinear predictor in this paper. The MLP \tilde{f} [29] which is composed of three-layers (d -units in the input layer, d -units in the output layer, and h -units in the hidden layer) is given by

$$\tilde{f}(\Omega, X) = {}^T (\tilde{f}_1(\Omega, X), \tilde{f}_2(\Omega, X), \dots, \tilde{f}_d(\Omega, X)), \quad (2.9)$$

where

$$\tilde{f}_k(\Omega, X) = \sum_{j=1}^h \omega_{(k-1)h+j} \sigma \left(\sum_{i=1}^d \omega_{dh+(j-1)d+i} x_i + \omega_{2dh+j} \right) \quad (k = 1, 2, \dots, d),$$

$$\sigma(y) = \frac{2}{1 + e^{-y}} - 1, \quad \Omega = {}^T (\omega_1, \omega_2, \dots, \omega_L) \quad \text{with} \quad L = (2d + 1)h.$$

Using the MLP, the nonlinear predictor F is constructed as

$$F(\Omega, X) = X + \Delta t \tilde{f}(\Omega, X). \quad (2.10)$$

The parameters $\{\Omega(i)\}_{i=1,2,\dots,J}$ which correspond to the windowed trajectories $\{X_n(i)\}_{i=1,2,\dots,J}$ are computed as follows. First, J -windows of trajectories $\{X_n(i)\}_{i=1,2,\dots,J}$ are periodically ordered as

$$\{X_n(1)\}, \{X_n(2)\}, \dots, \{X_n(J)\}, \{X_n(J+1)\} (= \{X_n(1)\}), \dots. \quad (2.11)$$

Second, $\Omega(1)$ is computed by minimizing the cost function:

$$U(\Omega) = \sum_{n=1+(d-1)\tau}^{(d-1)\tau+T-K} \sum_{k=1}^K \frac{1}{2} \left| X_{n+k}(1) - F^k(\Omega, X_n(1)) \right|^2 \quad (2.12)$$

via the gradient-descent method¹ with a random initial condition $\Omega(1) \in [0, 1]^L$. Then, $\Omega(i)$ ($i = 2, 3, \dots$) is computed by minimizing the cost function (2.12) defined for the i th trajectory $\{X_n(i)\}$ in a similar manner as $\Omega(1)$ except that $\Omega(i-1)$ is selected as the initial condition instead of the random values.

The procedures for computing $\{\Omega(i)\}_{i=1,2,\dots}$ are repeated until they converge to a periodic sequence as

$$\Omega(N_J), \Omega(N_J + 1), \dots, \Omega(N_J + J), \Omega(N_J + J + 1) (= \Omega(N_J)), \dots \quad (2.13)$$

where N_J is assumed to be sufficiently large.

2.4. Extracting principal bifurcation parameters

From the nonlinear prediction parameters $\{\Omega(i)\}$, principal component parameters are extracted by the Karuhnen–Loève (KL) transform [31–34].

First, we consider the subsequence of the parameters $\{\Omega(i) | i = N_J, N_J + 1, \dots, N_J + N_K - 1\}$ (N_K : element number) and compute Ω_0 and $\{\delta\Omega_i | i = 1, 2, \dots, N_K\}$ as

$$\Omega_0 = \frac{1}{N_K} \sum_{i=1}^{N_K} \Omega(N_J + i - 1), \quad (2.14)$$

$$\delta\Omega_i = \Omega(N_J + i - 1) - \Omega_0. \quad (2.15)$$

Second, the multivariate distribution of $\{\delta\Omega_i | i = 1, 2, \dots, N_K\}$ is computed in terms of the covariance matrix:

$$\Omega_{L \times L} = \frac{1}{N_K} \sum_{i=1}^{N_K} \delta\Omega_i^T \delta\Omega_i. \quad (2.16)$$

Since $\Omega_{L \times L}$ has non-negative eigenvalues $\{\lambda_1, \lambda_2, \dots, \lambda_L\}$, they are arranged in descending order:

$$\lambda_1 \geq \lambda_2 \geq \dots \geq \lambda_L \geq 0. \quad (2.17)$$

Applying KL-transformation to $\delta\Omega$, the principal parameters are given by

$$\Gamma = (\gamma_1, \gamma_2, \dots, \gamma_L) = {}^T [u_1 | u_2 \dots | u_L]^{-1} \delta\Omega \quad (2.18)$$

where $\{u_1, u_2, \dots, u_L\}$ are the eigenvectors corresponding to $\{\lambda_1, \lambda_2, \dots, \lambda_L\}$.

Since the transformation (2.18) diagonalizes the covariance matrix (2.16) in Γ -space, the diagonal elements $\{\lambda_1, \lambda_2, \dots, \lambda_L\}$ represent the significance of their corresponding principal parameters $\{\gamma_1, \gamma_2, \dots, \gamma_L\}$. By computing the normalized eigenvalues

$$\Lambda_i = \frac{\lambda_i}{\sum_{j=1}^L \lambda_j} \quad (i = 1, 2, \dots, L), \quad (2.19)$$

¹ In our experiment, the cost function (2.12) is minimized by a single iteration of the gradient-descent procedure $\Omega' = \Omega - \alpha \nabla U(\Omega)$, where $\nabla U(\Omega)$ is a gradient vector and α is determined by the line-search method which minimizes $U(\Omega - \alpha \nabla U(\Omega))$. The gradient vector $\nabla U(\Omega)$ is computed by the recurrent back-propagation algorithm of [26,30].

and the cumulative significance ratio from the first to the k th principal components

$$\Theta_k = \sum_{i=1}^k \Lambda_i \quad (k = 1, 2, \dots, L) \quad (2.20)$$

the number of significant parameters M (empirically set as $\Theta_M > 0.98$) is determined.

With respect to the significant parameters Γ_M , the M -parameter family of nonlinear predictors is constructed as

$$X_{n+1} = F(\Omega(\Gamma_M), X_n), \quad (2.21)$$

where

$$\Omega(\Gamma_M) = {}^T [u_1 | u_2 | \dots | u_L]^{-1} [\Gamma_M | 0] + \Omega_0, \quad (2.22)$$

where 0 denotes $(L - M)$ -dimensional 0 column vector.

In the studies of [25,26], it has been shown that the principal parameter family of nonlinear predictors (2.21) exhibits qualitatively similar bifurcation phenomena as the original (2.1), where the original bifurcation parameters p are mapped to the principal parameters Γ_m via a homeomorphism $\psi : R^m \rightarrow R^m$. This implies that the switch dynamics in the original bifurcation parameters p can be detected in the principal parameter space of the nonlinear predictors (2.21).

2.5. Detection of switch points

In order to detect switch dynamics in the chaotic trajectory $\{X_n\}$, we characterize the temporal dynamics of the chaotic trajectory in terms of the principal bifurcation parameters Γ_M . Again, we divide the trajectory $\{X_n\}$ into Q -windows of shorter-term trajectories with S -interval:

$$\{X_n(i) = X_n | n = 1 + (d - 1)\tau + (i - 1)S, \dots, (d - 1)\tau + iS\}_{i=1,2,\dots,Q} \quad (2.23)$$

Then, each window of trajectory $\{X_n(i)\}$ is characterized by the principal bifurcation parameters $\Gamma_M(i)$ which approximate the trajectory dynamics as

$$X_{n+1}(i) \approx F(\Omega(\Gamma_M(i)), X_n(i)). \quad (2.24)$$

The principal parameters $\Gamma_M(i)$ can be computed by minimizing the cost function:

$$U(\Gamma_M) = \sum_{n=1+(d-1)\tau+(i-1)S}^{(d-1)\tau+iS-K} \sum_{k=1}^K \frac{1}{2} |X_{n+k}(i) - F^k(\Omega(\Gamma_M), X_n(i))|^2 \quad (2.25)$$

via the quasi-Newton method [35] with random initial condition $\Gamma_M \in [0, 1]^M$.

Finally, in order to determine the number of switch parameters I and to classify the sets of principal parameters $\{\Gamma_M(i) | i = 1, 2, \dots, Q\}$ into the corresponding switched parameters $\{p(i) | i = 0, 1, \dots, I - 1\}$, the LBG-clustering algorithm [36] is applied. The algorithm analyzes the distribution of the principal parameters $\{\Gamma_M(i) | i = 1, 2, \dots, Q\}$ and classify them into q -nonoverlapping subgroups $\{\Gamma_M(i) | i \in R_j\}_{j=0,1,\dots,q-1}$ ($R_j \neq \emptyset$, $\bigcup_{j=0}^{q-1} R_j = \{1, 2, \dots, Q\}$, $R_i \cap R_j = \emptyset$ for $i \neq j$), which minimizes the distortion function:

$$D_q(R_1, R_2, \dots, R_q) = \frac{1}{Q} \sum_{j=0}^{q-1} \sum_{i \in R_j} |\Gamma_M(i) - \hat{\Gamma}(j)|^2, \quad (2.26)$$

$$\Xi = \max_{(i,j)} |\Gamma_M(i) - \Gamma_M(j)|^2,$$

$$\hat{\Gamma}(j) = \frac{1}{N_j} \sum_{i \in R_j} \Gamma_M(i) \quad (N_j : \text{number of elements in } R_j),$$

where Ξ is a normalization constant and $\hat{\Gamma}(j)$ is the j th centroid.

Using the least number of clusters q_{opt} which provides sufficiently small distortion function D_q (empirically set as $D_{q_{\text{opt}}} < 0.01$), we can determine the number of the switch parameters and classify the principal parameters $\{\Gamma_M(i) | i = 1, 2, \dots, Q\}$ into the corresponding centroids $\{\hat{\Gamma}(i) | i = 0, 1, \dots, q_{\text{opt}} - 1\}$. If $q_{\text{opt}} = I$ and the switch centroids $\{\hat{\Gamma}(i) | i = 0, \dots, q_{\text{opt}} - 1\}$ have one-to-one correspondence with the original switch points $\{p(i) | i = 0, 1, \dots, I - 1\}$, the switch dynamics of $s(t)$ can be correctly detected. For our convenience, the detected switch centroids $\{\hat{\Gamma}(0), \hat{\Gamma}(1), \dots\}$ are denoted by binary signal $s' = 0, 1, \dots$, respectively. Of course, there is an indeterminacy in the permutation of the switch signal $s'(t)$ and exactly the same switch signal as the original $s(t)$ can not be usually recovered. The switch points are finally determined as the time when the switch signal $s'(t)$ changes into another signal as $s'(t) \neq s'(t + \Delta t)$.

3. Numerical experiments

In this section, we test our algorithm against three chaotic dynamical systems: the Lorenz equations [37], the Rössler equations [38], and the Mackey–Glass equations [39]. It is shown that the algorithm detects switch dynamics among two or three sets of bifurcation parameter values.

3.1. Lorenz equation

As a first example, we consider the Lorenz equations [37]:

$$\frac{d^1 \eta_t}{dt} = \sigma(2\eta_t - {}^1\eta_t), \quad \frac{d^2 \eta_t}{dt} = r^1 \eta_t - {}^2\eta_t - {}^1\eta_t {}^3\eta_t, \quad \frac{d^3 \eta_t}{dt} = {}^1\eta_t {}^2\eta_t - b(s(t)) {}^3\eta_t \quad (3.1)$$

In this experiment, parameter values for σ and r are fixed to

$$\sigma = 16, \quad r = 45.6,$$

and the bifurcation parameter b makes switches among two values,

$$b(0) = 4.4, \quad b(1) = 4, \quad (3.2)$$

according to the switch signal $s(t)$.

Let us analyze the switch dynamics of the Lorenz equations modulated by the square wave signal $s(t)$ of Fig. 1(a). The chaotic time-waveform is then obtained as

$$\{\xi_n = ({}^1\eta_{n\Delta t}/30) + v_n | n = 1, 2, \dots, N_{\text{data}}\}, \quad (3.3)$$

where the sampling rate, the number of the data, and the Gaussian noise level are set as $\Delta t = 0.02$, $N_{\text{data}} = 7200$, and $v_n \in N(0, 0.02)$. The Lorenz equation is numerically integrated by the fourth-order Runge–Kutta algorithm with a time step of 0.001.

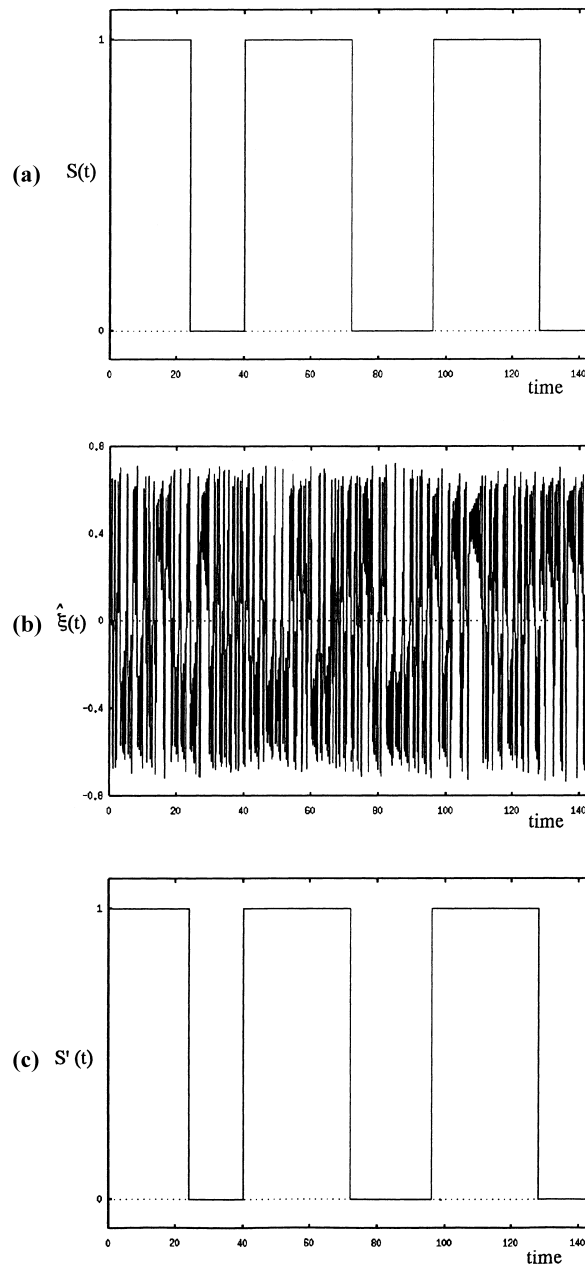


Fig. 1. (a) Switch signal $s(t)$ of the bifurcation parameter b in the Lorenz equation (3.1). (b) Average-filtered time-waveform $\{\hat{\xi}_n\}$ (2.5) recorded from the switched Lorenz equation. (c) Switch signal $s'(t)$ predicted by the present algorithm.

Fig. 1(b) shows the average-filtered time-waveform $\{\hat{\xi}_n\}$ with the averaging window length of $W = 7$. While the observational noise has been smoothed out by the average filter, it is difficult to recognize qualitative change in the switched chaotic time-waveform.

When the switch dynamics takes place among chaotic attractors with distinctively different geometric structure, it is reported in [15] that the switch dynamics are discernible in the maximum recurrent plots of the time-waveform. The

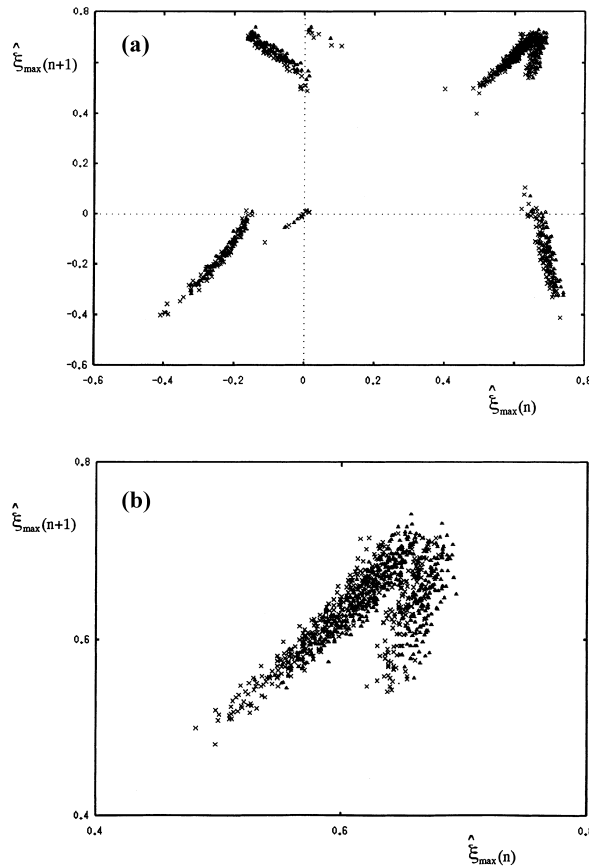


Fig. 2. (a) Maximum recurrent plots $(\hat{\xi}_{\max}(n), \hat{\xi}_{\max}(n+1))$ of the average-filtered time-waveform of Fig. 1(b). The crosses indicate the maximum plots of the Lorenz equation (3.1) with $b = 4.0$ and the triangles indicate the maximum plots of the Lorenz equation with $b = 4.4$. (b) Enlargement of (a) with $(\hat{\xi}_{\max}(n), \hat{\xi}_{\max}(n+1)) \in [0.4, 0.8] \times [0.4, 0.8]$.

maximum plots display the geometric difference of the switching attractors and indicate the switch dynamics which falls in either branch of the distinctive attractors. Fig. 2 shows the maximum plots obtained from the average-filtered time-waveform $\{\hat{\xi}_n\}$ of Fig. 1(b). Whereas the two chaotic attractors with $b = 4.4$ and $b = 4$ may have rather different geometric structures, the observational noise thickens their sheet geometries and mixes the domains of the switching attractors. Hence, it is hard to distinguish the attractors and to detect the switching points in the presence of noise. As the number of the switching attractors increases further, systematic detection of switching attractors by simple maximum plots may become much more difficult.

Let us test our algorithm. First, three-dimensional trajectory $\{X_n | n = 1 + (d-1)\tau, \dots, N - W\}$ ($d = 3, \tau = 4$) is reconstructed from the filtered time-waveform $\{\hat{\xi}_n\}$. The trajectory $\{X_n\}$ is divided into 6-windows of trajectories $\{X_n(i)\}_{i=1,2,\dots,6}$ with a time interval of $T = 1200$.

Second, using the nonlinear predictors defined by Eq. (2.10) with $h = 10$, we seek the parameters $\{\Omega(1), \Omega(2), \dots\}$ corresponding to

$$\{X_n(1)\}, \{X_n(2)\}, \dots, \{X_n(6)\}, \{X_n(7)\}, (= \{X_n(1)\}), \dots \tag{3.4}$$

by minimizing the cost function defined by Eq. (2.12) with $K = 2$.

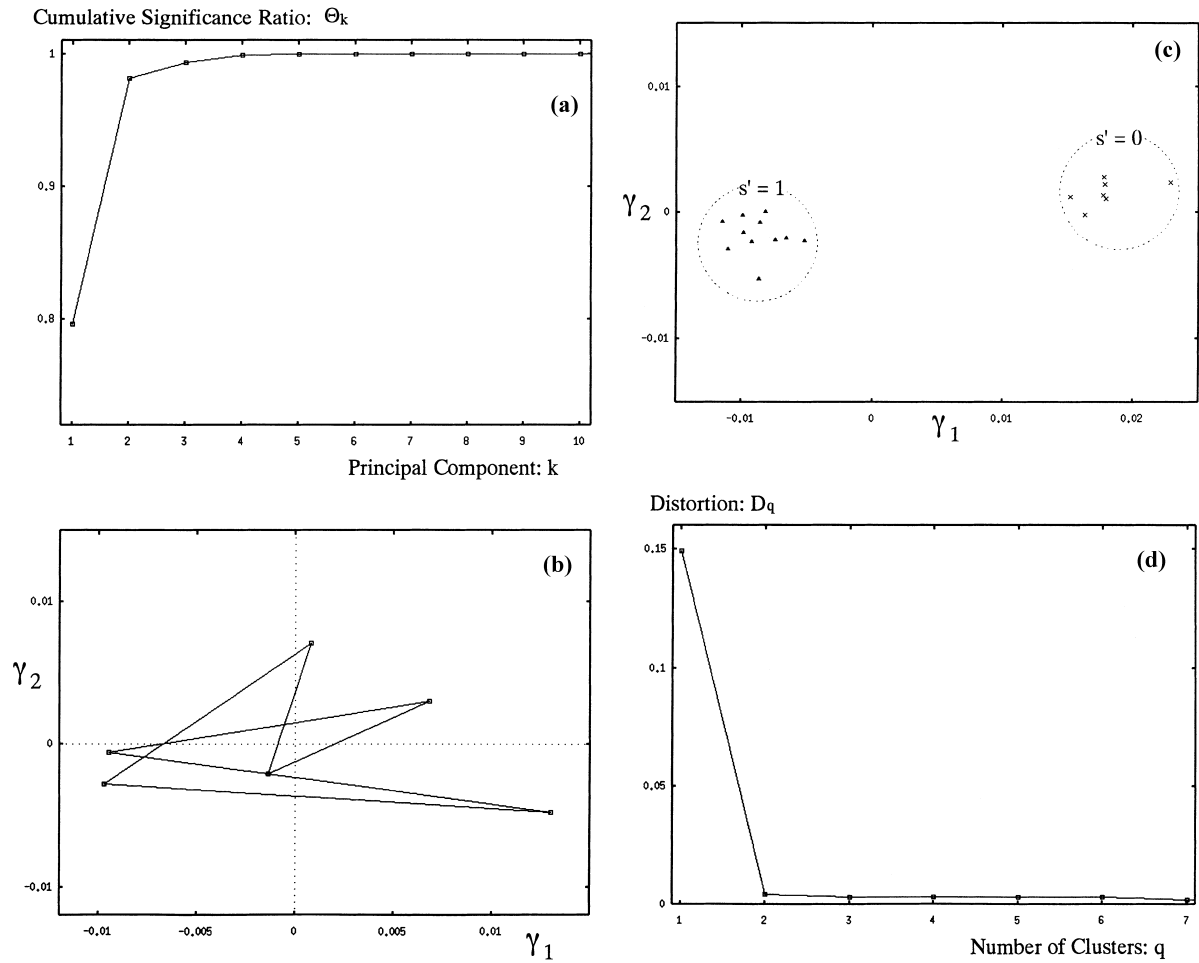


Fig. 3. (a) Cumulative significance ratio $\{\Theta_k\}$ of the covariance matrix (2.16). (b) Locations of the subsequence $\{\Omega(9988), \dots, \Omega(9999)\}$ of the nonlinear prediction parameters in the two-dimensional principal space (γ_1, γ_2) . (c) Locations of the principal parameter values $\{\Gamma_2(i)\}_{i=1,2,\dots,18}$ corresponding to the windows of short-term trajectories $\{X_n(i)\}_{i=1,2,\dots,18}$. The principal parameters are classified into two-groups, where the crosses indicate the points classified into “ $s' = 0$ ” and the triangles indicate the points classified into “ $s' = 1$ ”. (d) Distortion function D_q (2.27) optimized by the LBG-clustering algorithm with a cluster number q .

Third, we extract effective parameters $\{\gamma_1, \gamma_2, \dots\}$ of Ω by the principal component analysis applied to subsequence $\{\Omega(9988), \Omega(9989), \dots, \Omega(9999)\}$. Fig. 3 (a) shows the cumulative significance ratio Θ_k of the covariance matrix ((2.16)). Since $\Theta_2 > 0.98$, we set the principal component parameters as $\Gamma_2 = (\gamma_1, \gamma_2)$. Fig. 3(b) shows the locations of the subsequence of the parameters $\{\Omega(9988), \dots, \Omega(9999)\}$ in the (γ_1, γ_2) -space.

Fourth, the trajectory $\{X_n\}$ is divided again into 18-windows of shorter trajectories $\{X_n(i)\}_{i=1,2,\dots,18}$ with a time interval of $S = 400$. In Fig. 3(c), the trajectories $\{X_n(i)\}_{i=1,2,\dots,18}$ are characterized by the principal parameter values $\{\Gamma_2(i)\}_{i=1,2,\dots,18}$ which minimize the cost functions (2.25). The switch dynamics among the two-clusters of distinctive points in principal parameter space is clearly recognized. It is indeed shown in Fig. 3(d) that the LBG-clustering is optimized by the cluster number of $q_{\text{opt}} = 2$ which gives a sufficiently small distortion function $D_2 < 0.01$. Fig. 1(c) shows the sequence of the LBG-clustering signal $s'(t)$, which predicts the original signal $s(t)$ with good accuracy. Hence, systematic detection of the number of switch dynamics as well as their switch points is realized by the present algorithm.

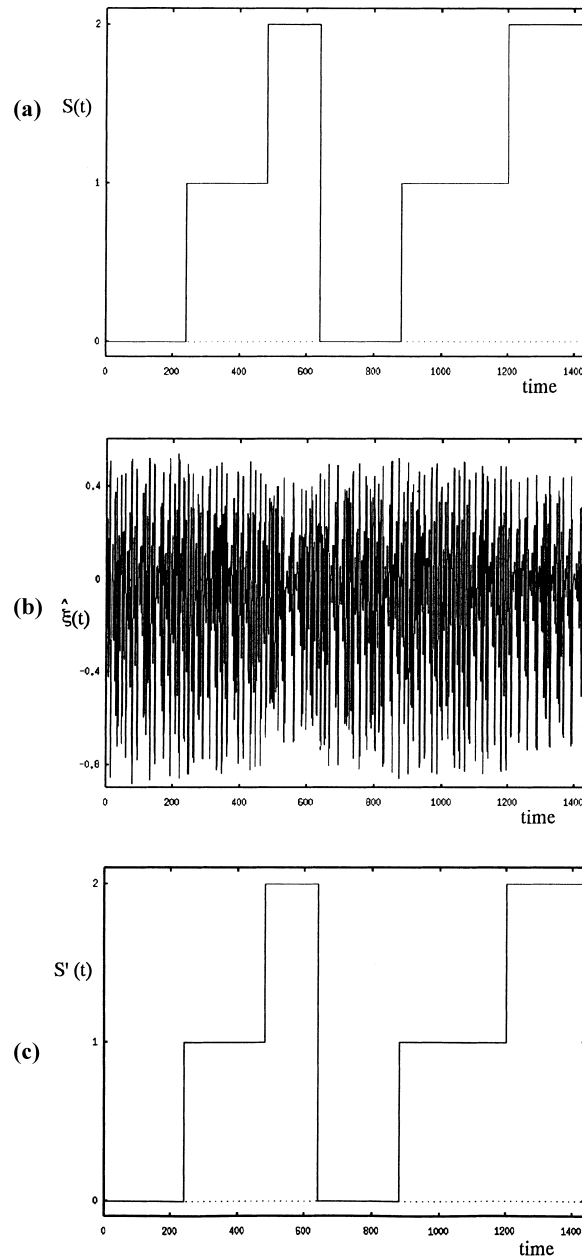


Fig. 4. (a) Switch signal $s(t)$ of the bifurcation parameters (a, c) in the Rössler equation (3.5). (b) Average-filtered time-waveform $\{\hat{\xi}_n\}$ from the switched Rössler equation. (c) Switch signal $s'(t)$ predicted by the present algorithm.

It should be noted that, in the present experiment, switch in the bifurcation parameters does not occur within any window of shorter-term chaotic trajectory. If a switch occurs within a window, the principal parameter values Γ_2 corresponding to the window cannot be accurately estimated. If such a switch occurs frequently and if the principal parameter values cannot be accurately estimated for many windows, identification of the number of the switch dynamics as well as their switch points may become quite difficult. We consider, however, that if the switch

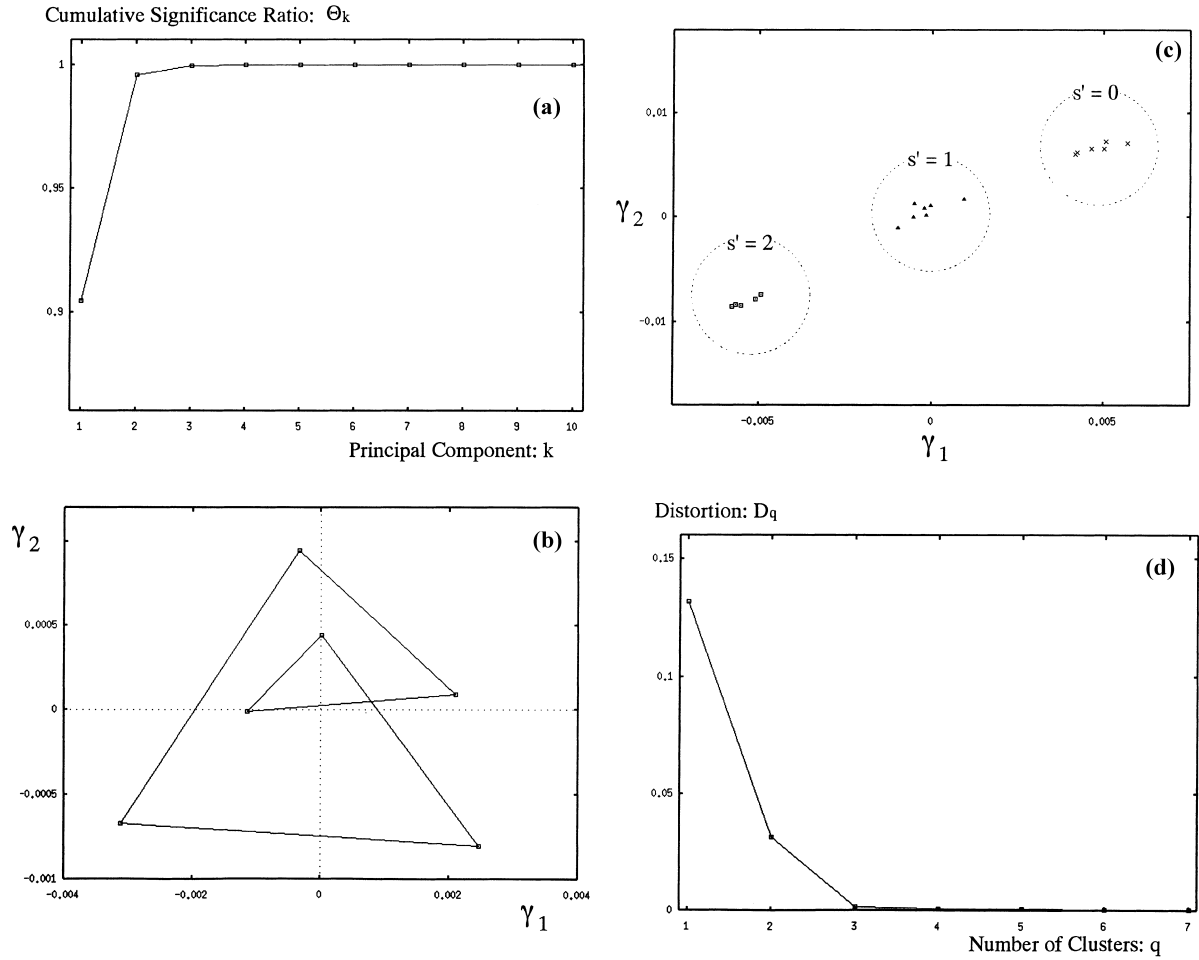


Fig. 5. (a) Cumulative significance ratio $\{\Theta_k\}$. (b) Locations of the subsequence $\{\Omega(9988), \dots, \Omega(9999)\}$ of the nonlinear prediction parameters in the two-dimensional principal space (γ_1, γ_2) . (c) Locations of the principal parameter values $\{\Gamma_2(i)\}_{i=1,2,\dots,18}$ corresponding to the windows of short-term trajectories $\{X_n(i)\}_{i=1,2,\dots,18}$. The principal parameters are classified into three-groups, where the crosses indicate the points classified into “ $s' = 0$,” the triangles indicate the points classified into “ $s' = 1$,” and the squares indicate the points classified into “ $s' = 2$ ”. (d) Distortion function D_q optimized by the LBG-clustering algorithm with a cluster number q .

occurs only intermittently and if the bifurcation parameters rarely change within a window, reliable estimation of the principal bifurcation parameters is possible for “most” of the windows of chaotic trajectories. Hence, for such intermittent switch signal, the present algorithm may identify the number of switch dynamics with good accuracy.

3.2. Rössler equation

As a second example, we consider the Rössler equations [38]:

$$\frac{d^1 \eta_t}{dt} = -2\eta_t - 3\eta_t, \quad \frac{d^2 \eta_t}{dt} = {}^1 \eta_t + a(s(t)) {}^2 \eta_t, \quad \frac{d^3 \eta_t}{dt} = b^1 \eta_t - (c(s(t)) - {}^1 \eta_t)^3 \eta_t, \quad (3.5)$$

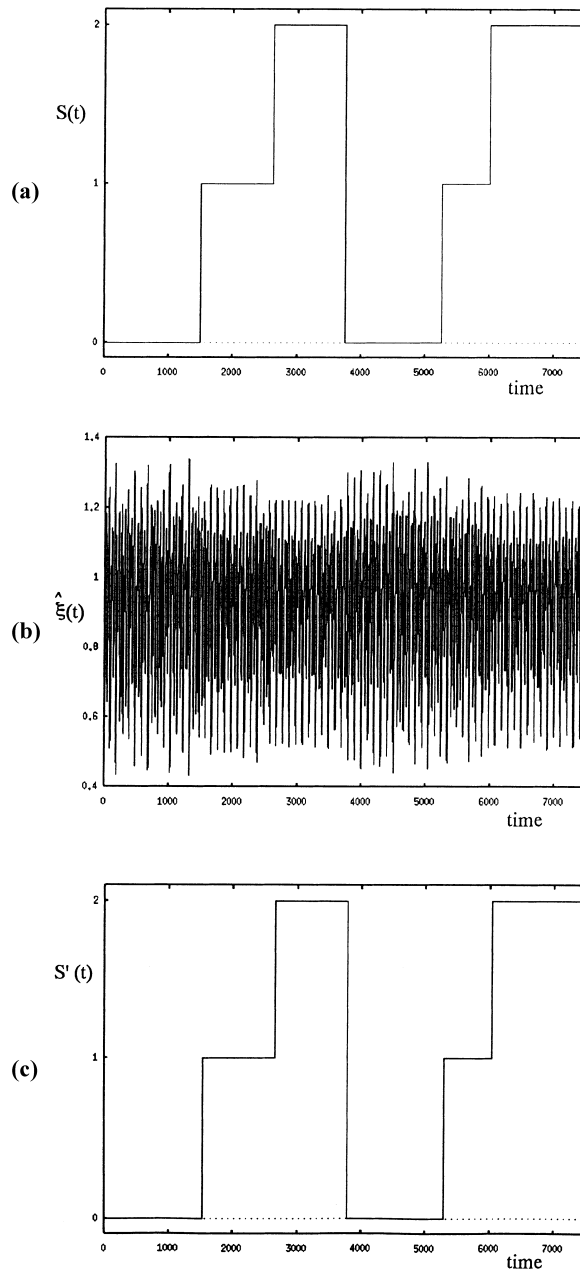


Fig. 6. (a) Switch signal $s(t)$ of the bifurcation parameter a of the Mackey–Glass equation (3.8). (b) Average-filtered time-waveform $\{\hat{\xi}_n\}$ from the switched Mackey–Glass equation. (c) Switch signal $s'(t)$ predicted by the present algorithm.

where the parameter value b is fixed as $b = 0.3$ and the bifurcation parameters (a, c) take three sets of values:

$$(a(0), c(0)) = (0.34, 5.6), \quad (a(1), c(1)) = (0.36, 5.2), \quad (a(2), c(2)) = (0.34, 4.8), \quad (3.6)$$

according to the switch signal $s(t)$ of Fig. 4(a). The chaotic time-waveform is obtained as

$$\{\xi_n = (\eta_n^2/10) + \nu_n | n = 1, 2, \dots, N_{\text{data}}\}, \quad (3.7)$$

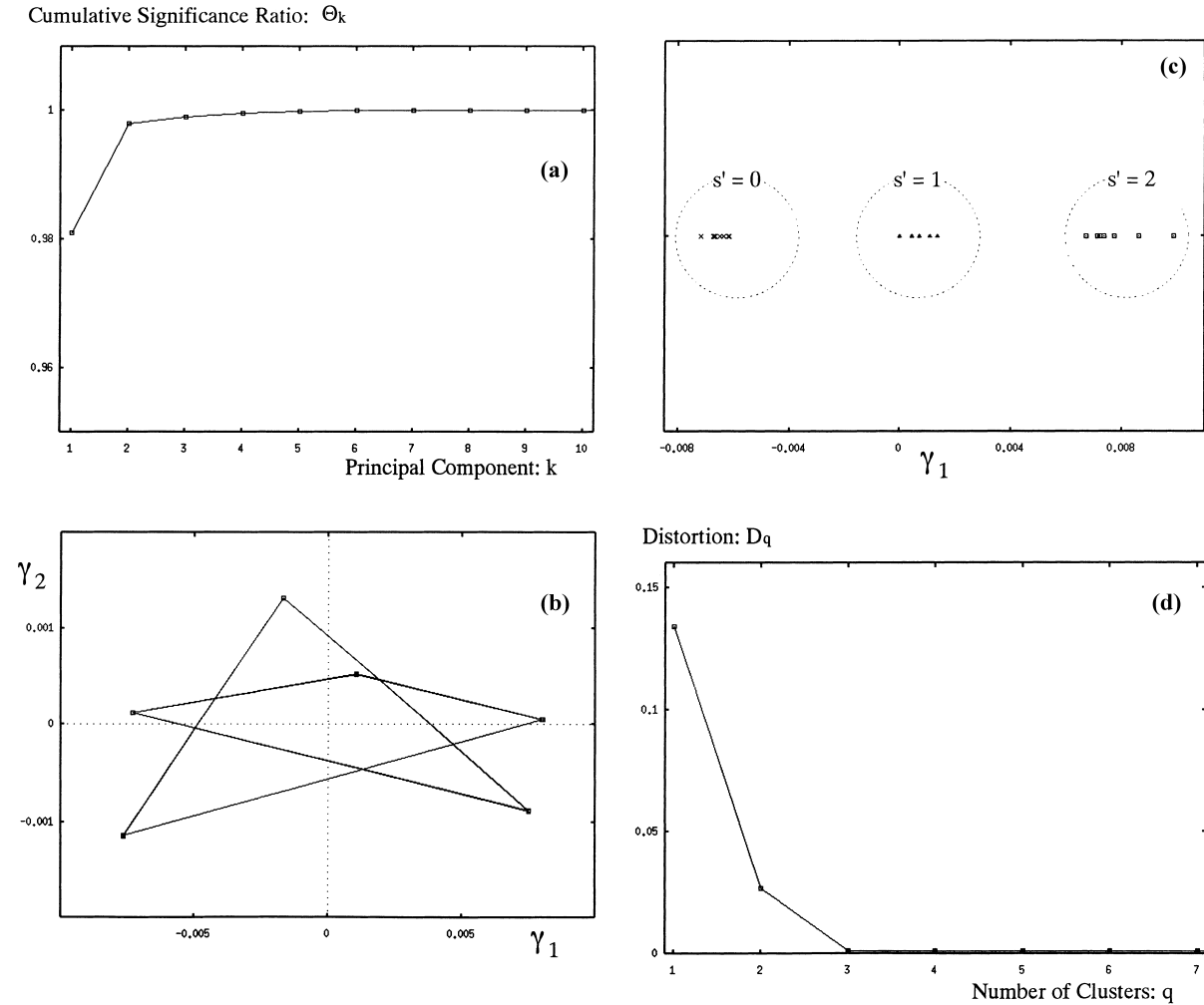


Fig. 7. (a) Cumulative significance ratio $\{\Theta_k\}$. (b) Locations of the subsequence $\{\Omega(9988), \dots, \Omega(9999)\}$ of the nonlinear prediction parameters in the one-dimensional principal space (γ_1). (c) Locations of the principal parameter values $\{\Gamma_1(i)\}_{i=1,2,\dots,20}$ corresponding to the windows of short-term trajectories $\{X_n(i)\}_{i=1,2,\dots,20}$. The principal parameters are classified into three-groups, where the crosses indicate the points classified into “ $s' = 0$,” the triangles indicate the points classified into “ $s' = 1$,” and the squares indicate the points classified into “ $s' = 2$.” (d) Distortion function D_q optimized by the LBG-clustering algorithm with a cluster number q .

where $\Delta t = 0.2$, $N_{\text{data}} = 7200$, $v_n \in N(0.0, 0.02)$, and the Rössler equation is numerically integrated by the fourth-order Runge–Kutta algorithm with a time step of 0.01.

Figs. 4 and 5 show the results of the detection algorithm. The parameters of the algorithm are set as $(W, d, \tau, J, T, h, K, N_J, N_K) = (5, 3, 4, 6, 1200, 8, 2, 9988, 12)$. According to the principal component analysis of Fig. 5(a), cumulative significance ratio of $\Theta_2 > 0.98$ is obtained. Hence, we set the principal component parameters as $\Gamma_2 = (\gamma_1, \gamma_2)$. Fig. 5(c) shows the locations of the principal parameter values $\{\Gamma_2(i)\}_{i=1,2,\dots,18}$ corresponding to the 18-windows of shortly divided trajectories $\{X_n(i)\}_{i=1,2,\dots,18}$ with a time interval of $S = 400$. The switch dynamics among the 3-clusters of distinctive points in principal parameter space is clearly recognized. According to the LBG-clustering analysis of Fig. 5(d), it is shown that the optimal cluster number is $q_{\text{opt}} = 3$. As in Fig. 4(c), the switch signal $s'(t)$ of the LBG-cluster data accurately predicts the original signal $s(t)$.

3.3. Mackey–Glass equation

As a final example, we consider the Mackey–Glass difference–differential equation [39]:

$$\frac{d\eta_t}{dt} = a(s(t)) \frac{\eta_{t-17}}{1 + \eta_{t-17}^{10}} - 0.1\eta_t. \quad (3.8)$$

The bifurcation parameter a takes three values:

$$a(0) = 0.21, \quad a(1) = 0.2, \quad a(2) = 0.19, \quad (3.9)$$

according to the switch signal $s(t)$ of Fig. 6(a) and the corresponding chaotic time-waveform is obtained as

$$\{\xi_n = \eta_{n\Delta t} + v_n | n = 1, 2, \dots, N_{\text{data}}\}, \quad (3.10)$$

where $\Delta t = 1.25$, $N_{\text{data}} = 6000$, $v_n \in N(0, 0.02)$, and the Mackey–Glass equation is numerically integrated by the fourth-order Runge–Kutta algorithm with a time step of 0.025.

Figs. 6 and 7 show the results of the detection algorithm for the switch dynamics of the Mackey–Glass equation. The parameters of the algorithm are set as $(W, d, \tau, J, T, h, K, N_J, N_K) = (7, 4, 8, 6, 1000, 5, 2, 9988, 12)$. According to the principal component analysis of Fig. 7(a), cumulative significance ratio of $\Theta_1 > 0.98$ is obtained. Hence, we set the principal component parameters as $\Gamma_1 = (\gamma_1)$. Fig. 7(c) shows the locations of the principal parameter values $\{\Gamma_1(I)\}_{i=1,2,\dots,20}$ corresponding to the 20-windows of shortly divided trajectories $\{X_n(i)\}_{i=1,2,\dots,20}$ with a time interval of $S = 300$. Switch dynamics among the three-clusters of distinctive points in the principal parameter space is discernible. According to the LBG-clustering analysis of Fig. 7(d), optimal cluster number is correctly detected as $q_{\text{opt}} = 3$ and the original signal $s(t)$ can be accurately predicted by the LBG signal $s'(t)$ in Fig. 6(c).

4. Conclusions and discussions

We have presented an algorithm for detecting switch dynamics in chaotic time-waveform. By the switch dynamics, we mean that the bifurcation parameter values are occasionally changed in the chaotic time-waveform. Using three chaotic dynamical systems, the Lorenz equations, the Rössler equations, and the Mackey–Glass equations, whose bifurcation parameters switch among two or three sets of slightly different parameter values, efficiency of the algorithm is shown. For the chaotic time-waveforms contaminated with observational noise, our algorithm have accurately detected the number of switching parameters as well as their switching points.

It should be noted that the present algorithm is based upon the characterization of windows of short-term chaotic time-waveforms in terms of the principal bifurcation parameters of nonlinear predictors. Performance of the algorithm to identify the number of switching parameters and their switching points is primarily dependent upon a reliable estimation of the principal bifurcation parameter values corresponding to each window of chaotic time-waveform. Reliable estimation of the corresponding principal parameters becomes difficult when:

1. The observational noise level is quite high.
2. The window length of chaotic time-waveform is too short.
3. The bifurcation parameters frequently make switches within a window of chaotic time-waveform.

Exact number of the switching parameters may be accurately identified when the problems (1)–(3) are not so significant.

Limitation of the present algorithm against these problems will be studied in our future works. Applicability of the algorithm against higher-dimensional dynamical systems such as the spatio-temporal dynamical systems [12,40] would be also considered in our further studies.

Acknowledgements

The authors would like to thank Professor K. Aihara, Dr. T. Ikeguchi, and Dr. T. Schreiber for stimulating discussions and valuable comments on the present work. They would also like to thank one of the referees for careful and beneficial comments on the original manuscript.

References

- [1] H.D.I. Abarbanel, R. Brown, J.J. Sidorowich, L.S. Tsimring, The analysis of observed chaotic data in physical systems, *Rev. Mod. Phys.* 65(4) (1993) 1331.
- [2] P. Grassberger, I. Procaccia, Measuring the strangeness of strange attractors, *Physica D* 9 (1983) 189.
- [3] A. Wolf, J.B. Swift, H.L. Swinney, J.A. Vastano, Determining Lyapunov exponents from a time series, *Physica D* 16 (1985) 285.
- [4] M. Sano, Y. Sawada, Measurement of the Lyapunov spectrum from chaotic time series, *Phys. Rev. Lett.* 55 (1985) 1082.
- [5] J.P. Eckmann, S.O. Kamphorst, D. Ruelle, S. Ciliberto, Lyapunov exponents from a time series, *Phys. Rev. A* 34(6) (1986) 4971.
- [6] A.M. Fraser, Information and entropy in strange attractors, *IEEE Trans. Info. Theor.* 35 (1989) 245.
- [7] J.P. Crutchfield, B.S. McNamara, Equations of motion from a data series, *Complex Systems* 1 (1987) 417.
- [8] J.D. Farmer, J.J. Sidorowich, Predicting chaotic time series, *Phys. Rev. Lett.* 59 (1987) 845.
- [9] A. Lapedes, R. Farber, Nonlinear signal processing using neural networks, Tech. Rep. Los Alamos National Lab. (1987) LA-UR-87-2662.
- [10] M. Casdagli, Nonlinear prediction of chaotic time series, *Physica D* 35 (1989) 335.
- [11] G. Sugihara, R.M. May, Nonlinear forecasting as a way of distinguishing chaos from measurement error in time series, *Nature* 344 (1990) 734.
- [12] M.C. Cross, P.C. Hohenberg, Pattern formation outside of equilibrium, *Rev. Mod. Phys.* 65(3) (1993) 851.
- [13] K.M. Cuomo, A.V. Oppenheim, Circuit implementation of synchronized chaos with applications to communications, *Phys. Rev. Lett.* 71(1) (1993) 65.
- [14] H. Dedieu, M.P. Kennedy, M. Hasler, Chaos shift keying, *IEEE Trans. CAS* 40(10) (1993) 634.
- [15] G. Pérez, H.A. Cerdeira, Extracting messages masked by chaos, *Phys. Rev. Lett.* 74(11) (1995) 1970.
- [16] L.M. Pecora, T.L. Carroll, Synchronization in chaotic systems, *Phys. Rev. Lett.* 64(8) (1990) 821.
- [17] T.L. Carroll, L.M. Pecora, Synchronizing chaotic circuits, *IEEE Trans. CAS* 38(4) (1991) 453.
- [18] H. Isliker, J. Kurths, A test for stationarity, *Int. J. Bifurcation and Chaos* 3(6) (1993) 1573.
- [19] R. Manuca, R. Savit, Stationarity and nonstationarity in time series analysis, *Physica D* 99 (1996) 134.
- [20] M.C. Casdagli, Recurrence plots revisited, *Physica D* 108 (1997) 12.
- [21] T. Schreiber, Detecting and analyzing nonstationarity in a time series using nonlinear cross predictions, *Phys. Rev. Lett.* 78(5) (1997) 843.
- [22] T. Schreiber, A. Schmitz, Classification of time series data with nonlinear similarity measures, *Phys. Rev. Lett.* 79(8) (1997) 1475.
- [23] M.B. Kennel, Statistical test for dynamical nonstationarity in observed time series data, *Phys. Rev. E* 56(1) (1997) 316.
- [24] A. Witt, J. Kurths, A. Pikovsky, Testing stationarity in time series, *Phys. Rev. E* 58(2) (1998) 1800.
- [25] R. Tokunaga, S. Kajiwara, T. Matsumoto, Reconstructing bifurcation diagrams only from time-waveforms, *Physica D* 79 (1994) 348.
- [26] I. Tokuda, S. Kajiwara, R. Tokunaga, T. Matsumoto, Recognizing chaotic time-waveforms in terms of a parametrized family of nonlinear predictors, *Physica D* 95 (1996) 380.
- [27] F. Takens, Detecting strange attractors in turbulence, in: *Lecture Notes in Mathematics*, vol. 898 Springer, Berlin, 1981, p. 366.
- [28] T. Sauer, J.A. York, M. Casdagli, Embedology, *J. Stat. Phys.* 65(3) (1991) 579.
- [29] D.E. Rumelhart, J.L. McClelland, and the PDP Research Group, *Parallel Distributed Processing*, MIT Press, Cambridge, 1986.
- [30] R.J. Williams, D. Zipser, A Learning algorithm for continually running fully recurrent neural networks, *Neur. Comput.* 1 (1989) 270.
- [31] T.W. Anderson, *An Introduction to Multivariate Statistical Analysis*, Wiley, New York, 1958.
- [32] D.S. Broomhead, G.P. King, Extracting qualitative dynamics from experimental data, *Physica D* 20 (1986) 217.
- [33] A.M. Albano, J. Muench, C. Schwartz, A.I. Mees, P.E. Rapp, Singular-value decomposition and the Grassberger–Procaccia algorithm, *Phys. Rev. A* 38(6) (1988) 3017.
- [34] A.I. Mees, P.E. Rapp, L.S. Jennings, Singular-value decomposition and embedding dimension, *Phys. Rev. A* 36(1) (1987) 341.
- [35] D.G. Luenberger, *Linear and Nonlinear Programming*, Addison-Wesley, Reading, MA, 1973.
- [36] Y. Linde, A. Buzo, R. Gray, An algorithm for vector quantizer design, *IEEE Trans. Comm.* COM-28-1 (1980) 84.
- [37] E.N. Lorenz, Deterministic nonperiodic flow, *J. Atmos. Sci.* 20 (1963) 901.
- [38] O.E. Rössler, Continuous chaos, *Ann. N.Y. Acad. Sci.* 31 (1979) 376.
- [39] M.C. Mackey, L. Glass, Oscillation and chaos in physiological control systems, *Science* 197 (1977) 287.
- [40] K. Kaneko, Pattern dynamics in spatiotemporal chaos, *Physica D* 34 (1989) 1.